

Spatially Resolving the Quasar Broad Emission Line Region

GRAVITY Collaboration

Roberto Abuter⁸
 Matteo Accardo⁸
 Tobias Adler³
 António Amorim⁶
 Narsireddy Anugu^{7,29,30}
 Gerardo Ávila⁸
 Michi Bauböck¹
 Myriam Benisty^{5,12}
 Jean-Philippe Berger⁵
 Joachim M. Bestenlehner^{22,3}
 Hervé Beust⁵
 Nicolas Blind⁹
 Mickaël Bonnefoy⁵
 Henri Bonnet⁸
 Pierre Bourget⁸
 Jérôme Bouvier⁵
 Wolfgang Brandner³
 Roland Brast⁸
 Alexander Buron¹
 Leonard Burtscher¹⁴
 Faustine Cantalloube³
 Alessio Caratti o Garatti^{16,3}
 Paola Caselli¹
 Frédéric Cassaing¹⁰
 Frédéric Chapron²
 Benjamin Charnay²
 Élodie Choquet³⁷
 Yann Clénet²
 Claude Collin²
 Vincent Coudé du Foresto²
 Ric Davies¹
 Casey Deen¹
 Françoise Delplancke-Ströbele⁸
 Roderick Dembeter⁸
 Frédéric Derie⁸
 Willem-Jan de Wit⁸
 Jason Dexter¹
 Tim de Zeeuw^{1,14}
 Catherine Dougados⁵
 Guillaume Dubus⁵
 Gilles Duvert⁵
 Monica Ebert³
 Andreas Eckart^{4,13}
 Frank Eisenhauer¹
 Michael Esselborn⁸
 Fabio Eupen⁴
 Pierre Fédou²
 Miguel C. Ferreira⁶
 Gert Finger⁸
 Natascha M. Förster Schreiber¹
 Feng Gao¹
 César Enrique García Dabó⁸
 Rebeca García Lopez^{16,3}
 Paulo J. V. Garcia⁷
 Éric Gendron²
 Reinhard Genzel^{1,15}
 Ortwin Gerhard¹
 Juan Pablo Gil⁸
 Stefan Gillessen¹
 Frédéric Gonté⁸
 Paulo Gordo⁶
 Damien Gratadour²
 Alexandra Greenbaum⁴⁰
 Rebekka Grellmann⁴
 Ulrich Grözinger³
 Patricia Guajardo⁸
 Sylvain Guieu⁵
 Maryam Habibi¹
 Pierre Haguenaer⁸
 Oliver Hans¹
 Xavier Haubois⁸
 Marcus Haug⁸
 Frank Haußmann¹
 Thomas Henning³
 Stefan Hippler³
 Sebastian F. Hönig²⁷
 Matthew Horrobin⁴
 Armin Huber³
 Zoltan Hubert⁵
 Norbert Hubin⁸
 Christian A. Hummel⁸
 Gerd Jakob⁸
 Annemieke Janssen³⁶
 Alejandra Jimenez Rosales¹
 Lieselotte Jochum⁸
 Laurent Jocou⁵
 Jens Kammerer^{8,41}
 Martina Karl^{20,21}
 Andreas Kaufer⁸
 Stefan Kellner¹
 Sarah Kendrew^{11,3}
 Lothar Kern⁸
 Pierre Kervella²
 Mario Kiekebusch⁸
 Makoto Kishimoto³¹
 Lucia Klarmann³
 Ralf Klein³
 Rainer Köhler³
 Yitping Kok¹
 Johann Kolb⁸
 Maria Koutoulaki^{16,19,3,8}
 Martin Kulas³
 Lucas Labadie⁴
 Sylvestre Lacour^{2,8}
 Anne-Marie Lagrange⁵
 Vincent Lapeyrière²
 Werner Laun³
 Bernard Lazareff⁵
 Jean-Baptiste Le Bouquin⁵
 Pierre Léna²
 Rainer Lenzen³
 Samuel Lévêque⁸
 Chien-Cheng Lin^{3,18}
 Magdalena Lippa¹
 Dieter Lutz¹
 Yves Magnard⁵
 Anne-Lise Maire^{23,3}
 Leander Mehrgan⁸
 Antoine Mérand⁸
 Florentin Millour³⁷
 Paul Mollière³
 Thibaut Moulin⁵
 André Müller³
 Eric Müller^{8,3}
 Friedrich Müller³
 Hagai Netzer³²
 Udo Neumann³
 Mathias Nowak²
 Sylvain Oberti⁸
 Thomas Ott¹
 Laurent Pallanca⁸
 Johana Panduro³
 Luca Pasquini⁸
 Thibaut Paumard²
 Isabelle Percheron⁸
 Karine Perraut⁵
 Guy Perrin²
 Bradley M. Peterson^{24,25,26}
 Pierre-Olivier Petrucci⁵
 Andreas Pflüger¹
 Oliver Pfuhl⁸
 Than Phan Duc⁸
 Jaime E. Pineda¹
 Philipp M. Plewa¹
 Dan Popovic⁸
 Jörg-Uwe Pott³
 Almudena Prieto³⁹
 Laurent Pueyo¹¹
 Sebastian Rabien¹
 Andrés Ramírez⁸
 José Ricardo Ramos³
 Christian Rau¹
 Tom Ray¹⁶
 Miguel Riquelme⁸
 Gustavo Rodríguez-Coira²
 Ralf-Rainer Rohloff³
 Daniel Rouan²
 Gérard Rousset²
 Joel Sanchez-Bermudez^{3,17}
 Marc Schartmann^{1,33,34}
 Silvia Scheithauer³
 Markus Schöller⁸
 Nicolas Schuhler⁸
 Dominique Segura-Cox¹
 Jinyi Shangguan¹
 Thomas T. Shimizu¹
 Jason Spyromilio⁸
 Amiel Sternberg^{1,32}
 Matthias Raphael Stock²¹
 Odele Straub^{1,2}
 Christian Straubmeier⁴
 Eckhard Sturm¹
 Marcos Suárez Valles⁸
 Linda J. Tacconi¹
 Wing-Fai Thi¹

Konrad R. W. Tristram⁸
Javier J. Valenzuela⁸
Roy van Boekel³
Ewine F. van Dishoeck¹⁴
Pierre Vermot²
Frédéric Vincent²
Sebastiano von Fellenberg¹
Idel Waisberg¹
Jason J. Wang²⁸
Imke Wank⁴
Johannes Weber¹
Gerd Weigelt¹³
Felix Widmann¹
Ekkehard Wieprecht¹
Michael Wiest⁴
Erich Wieszorrek¹
Markus Wittkowski⁸
Julien Woillez⁸
Burkhard Wolff⁸
Pengqian Yang^{3,35}
Senol Yazici^{1,4}
Denis Ziegler²
Gérard Zins⁸

- ¹ Max Planck Institute for Extraterrestrial Physics, Garching, Germany
- ² LESIA, Observatoire de Paris, Université PSL, CNRS, Sorbonne Université, Université de Paris, Meudon, France
- ³ Max-Planck-Institut für Astronomie, Heidelberg, Germany
- ⁴ I Physikalisches Institut, Universität zu Köln, Germany
- ⁵ Univ. Grenoble Alpes, CNRS, IPAG, Grenoble, France
- ⁶ CENTRA and Universidade de Lisboa – Faculdade de Ciências, Lisboa, Portugal
- ⁷ CENTRA and Universidade do Porto – Faculdade de Engenharia, Porto, Portugal
- ⁸ ESO
- ⁹ Observatoire de Genève, Université de Genève, Versoix, Switzerland
- ¹⁰ DOTA, ONERA, Université Paris-Saclay, Châtillon, France
- ¹¹ European Space Agency, Space Telescope Science Institute, Baltimore, USA
- ¹² Unidad Mixta Internacional Franco-Chilena de Astronomía (CNRS UMI 3386), Departamento de Astronomía, Universidad de Chile, Las Condes, Santiago, Chile
- ¹³ Max Planck Institute for Radio Astronomy, Bonn, Germany
- ¹⁴ Sterrewacht Leiden, Leiden University, Leiden, the Netherlands

- ¹⁵ Department of Physics, Le Conte Hall, University of California, Berkeley, USA
- ¹⁶ Dublin Institute for Advanced Studies, Dublin, Ireland
- ¹⁷ Instituto de Astronomía, Universidad Nacional Autónoma de México, Ciudad de México, Mexico
- ¹⁸ Institute for Astronomy, University of Hawai'i, Honolulu, USA
- ¹⁹ School of Physics, University College Dublin, Ireland
- ²⁰ Max Planck Institute for Physics, Munich, Germany
- ²¹ TUM Department of Physics, Technical University of Munich, Garching, Germany
- ²² Department of Physics and Astronomy, University of Sheffield, UK
- ²³ STAR Institute, Liège, Belgium
- ²⁴ Department of Astronomy, The Ohio State University, Columbus, USA
- ²⁵ Center for Cosmology and AstroParticle Physics, The Ohio State University, Columbus, USA
- ²⁶ Space Telescope Science Institute, Baltimore, USA
- ²⁷ School of Physics & Astronomy, University of Southampton, UK
- ²⁸ Department of Astronomy, California Institute of Technology, Pasadena, USA
- ²⁹ Steward Observatory, Department of Astronomy, University of Arizona, Tucson, USA
- ³⁰ University of Exeter, School of Physics and Astronomy, Exeter, UK
- ³¹ Kyoto Sangyo University, Department of Astrophysics and Atmospheric Sciences, Japan
- ³² School of Physics and Astronomy, Tel Aviv University, Israel
- ³³ Excellence Cluster Origins, Ludwig-Maximilians-Universität München, Garching, Germany
- ³⁴ Universitäts-Sternwarte München, Munich, Germany
- ³⁵ Shanghai Institute of Optics and Fine Mechanics, Chinese Academy of Sciences, China
- ³⁶ NOVA Optical Infrared Instrumentation Group at ASTRON, Dwingeloo, the Netherlands
- ³⁷ Aix Marseille Univ, CNRS, CNES, LAM, France
- ³⁸ Observatoire de la Côte d'Azur Lagrange, Boulevard de l'Observatoire, Nice, France
- ³⁹ Instituto de Astrofísica de Canarias, La Laguna, Spain

- ⁴⁰ University of Michigan Department of Astronomy, Ann Arbor, USA
- ⁴¹ Research School of Astronomy & Astrophysics, Australian National University, Canberra, Australia

The angular resolution of the Very Large Telescope Interferometer (VLTI) and the excellent sensitivity of GRAVITY have led to the first detection of spatially resolved kinematics of high velocity atomic gas near an accreting supermassive black hole, revealing rotation on sub-parsec scales in the quasar 3C 273 at a distance of 550 Mpc. The observations can be explained as the result of circular orbits in a thick disc configuration around a 300 million solar mass black hole. Within an ongoing Large Programme, this capability will be used to study the kinematics of atomic gas and its relation to hot dust in a sample of quasars and Seyfert galaxies. We will measure a new radius-luminosity relation from spatially resolved data and test the current methods used to measure black hole mass in large surveys.

Introduction

Emission lines of atomic gas velocity-broadened to widths of 3000–10000 km s⁻¹ are a hallmark of quasars and are thought to trace the gravitational potential of the central supermassive black hole. Despite decades of study their physical origin remains unclear. The observed properties can be explained by emission from discrete, collapsed clouds or high-density regions of a continuous medium. The gas may be part of the inflow feeding the black hole or a continuous equatorial outflow. Assuming a gravitational origin, line widths combined with a measurement of the emission region size provide an estimate of the black hole mass.

Extensive monitoring campaigns use light echoes in a technique called reverberation mapping to measure the emission size, with ongoing work expanding the sample size from tens (Kaspi et al., 2000; Peterson et al., 2004) to hundreds (Du et al., 2016; Grier et al., 2017). The key result of these studies is that the size of the emitting region increases with

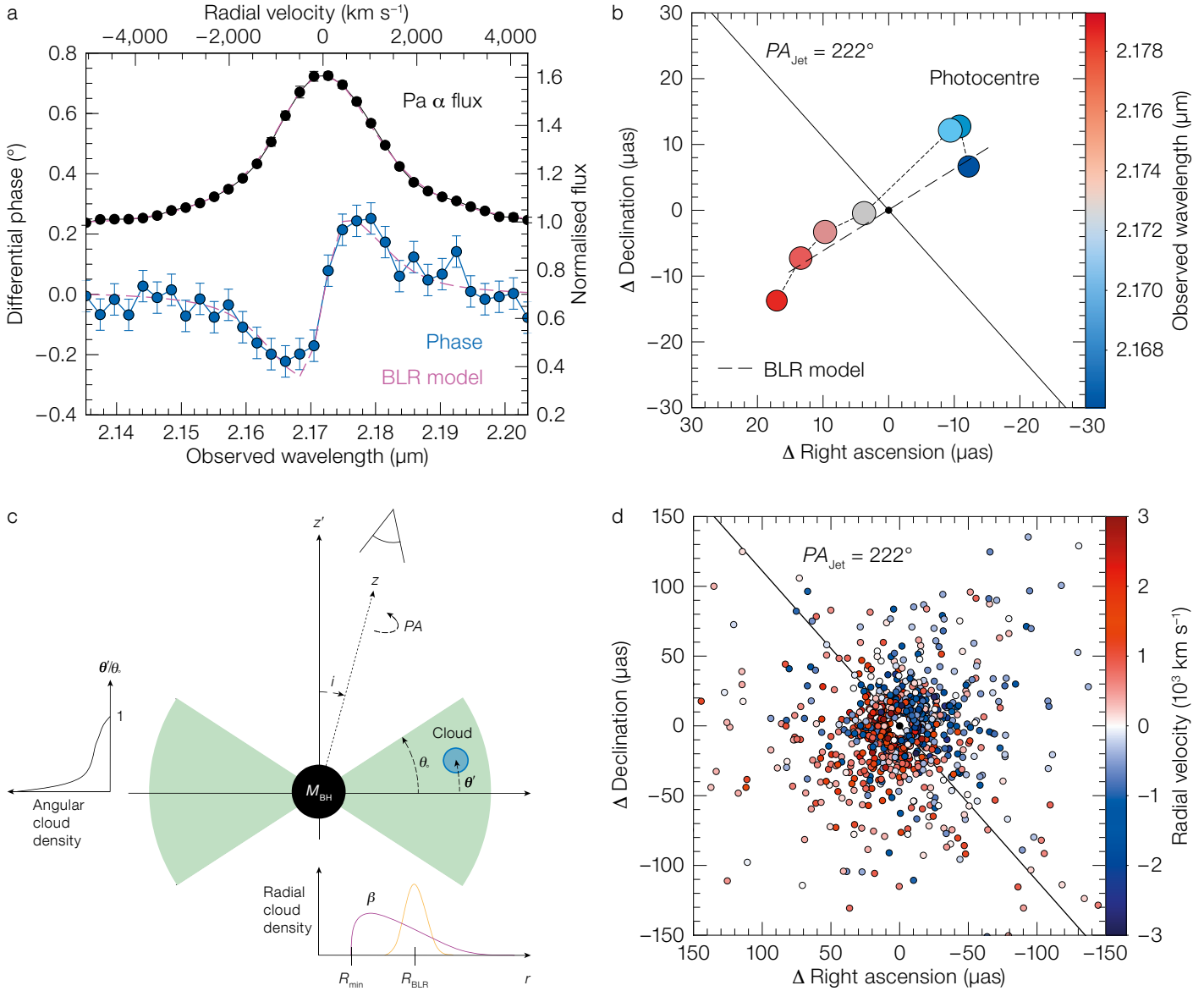


Figure 1. GRAVITY spatially resolves the broad emission line kinematics of 3C 273. (a) Pa α line profile (black) and averaged differential phase (blue), showing non-zero phases and a change of sign across the broad emission line. (b) Photocentre positions measured at each line channel, showing a clear separation between red and blue which corresponds to a velocity gradient at a position angle perpendicular to the large-scale radio jet of 3C 273 (black line).

This is the result of net ordered rotation of the line-emitting gas. By comparing a kinematic model of the emission region (c) to GRAVITY data, we find that a thick disc configuration viewed at low inclination best explains the data (d). The model also provides estimates of the mean emission radius and central black hole mass. Adapted from GRAVITY Collaboration (2018).

engines. The key components of AGN are small on the sky, at micro- to milli-arcsecond scales, requiring long baselines at the VLTI and Keck Interferometer. AGN are also relatively faint sources, so far only detected in optical interferometry with 8–10-metre-class telescopes and instrumentation with excellent sensitivity. Continuum measurements with the Keck Interferometer (for example, Kishimoto et al., 2011) and the Astronomical Multi-BEam combineR (AMBER) on the VLTI (Weigelt et al., 2012) provide information about hot dust surrounding the nucleus. The broad line region (BLR) is even smaller (angular size < 0.1 milliarcseconds [mas]) and is impossible to resolve in standard

luminosity, roughly as $R \sim L^{1/2}$. That relationship can be understood as atomic gas emission being produced under optimal photoionisation conditions (constant received flux). This radius-luminosity relation allows “secondary” methods for estimating black hole masses using a single optical spectrum (replacing long

campaigns to measure R via an estimate based on L). Secondary methods so far provide all available active galactic nucleus (AGN) black hole mass measurements in large samples and out to high redshift.

Interferometry provides an independent method for spatially resolving AGN central

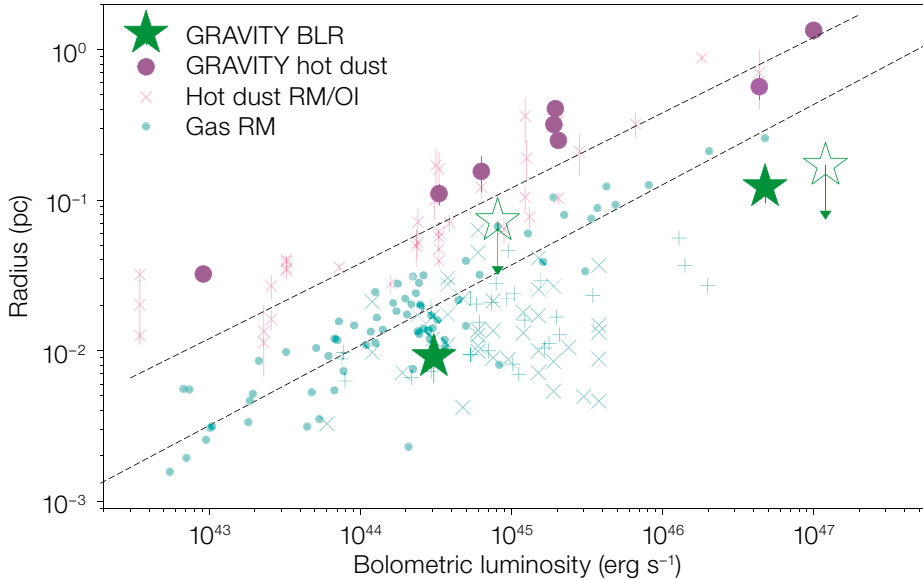


Figure 2. AGN radius-luminosity relationships measured for hot dust and atomic gas. The hot dust measurements include our new GRAVITY results (purple solid circles; see GRAVITY Collaboration, 2019a), as well as those from previous observations. For atomic gas, we have detected velocity gradients and measured the emission region size for the quasar 3C 273 (GRAVITY Collaboration, 2018) with another detection and upper limits in deep integrations for two other sources. With an ongoing large programme, we aim to expand the sample to roughly 10 AGN spanning four orders of magnitude in luminosity. The results can be compared to the large scatter found in reverberation mapping samples (different samples as smaller symbols) and to the $R \sim L^{0.5}$ relations found for both dust and atomic gas.

imaging, even with the VLTI. Instead, we can study its kinematics by measuring the photocentre shift of the atomic gas relative to the hot dust, as a function of wavelength (or velocity) across the emission line. The photocentre shift results in a small differential phase signal $\lesssim 1$ degree (Rakshit et al., 2015) whose detection requires high sensitivity and deep integrations. This is now possible with GRAVITY.

A case study in 3C 273

We observed 3C 273 with GRAVITY using the four Unit Telescopes (UTs) over eight nights between July 2017 and May 2018, with a total on-source integration time of 8 hours. By combining the data from all epochs, we measure the interferometric phase with a precision of ~ 0.1 – 0.2 degrees per baseline. An average of three of the six baselines shows the detection of an S-shaped phase signal, corresponding to a spatially resolved velocity gradient across the otherwise featureless broad $\text{Pa}\alpha$ emission line (Figure 1a). From the phase data, we fit for a model-independent photocentre position at wavelength channels where the line emission is strong. We find a clear separation between blue and red channels (a velocity gradient, Figure 1b), with an orientation perpendicular to the large-scale radio jet. This demonstrates net rotation of the line emission region. The photocentre positions are measured with a typical precision of 5 μas per channel.

By adopting a kinematic model of the $\text{Pa}\alpha$ emission region as a collection of orbiting gas clouds (following Pancoast et al., 2014 and Rakshit et al., 2015), we measure physical properties of the gas distribution and black hole. The data are consistent with a thick disc (opening angle of 45_{-6}^{+9} degrees) in Keplerian rotation around a supermassive black hole of 1.5 – $4.1 \times 10^8 M_{\odot}$. The inclination and position angles agree with those inferred for the radio jet. The measured mean emission radius of $R_{\text{BLR}} = 0.12 \pm 0.03$ pc (at an angular diameter distance of 548 Mpc) is a factor of about two smaller than reported in earlier RM studies (Kaspi et al., 2000; Peterson et al., 2004) although it is consistent with a recent one (Zhang et al., 2019). This first result supports the fundamental assumptions used in reverberation mapping and the secondary methods used to measure black hole mass. For more details, see GRAVITY Collaboration (2018).

Outlook

With an approved large programme we are carrying out observations of ~ 10 sources over the next two years, spanning four orders of magnitude in AGN luminosity. The data will provide information on the dominant kinematics and the degree of ordered motion in atomic gas in the broad emission line region, helping us to address the following questions: are the line widths pri-

marily set by rotation in the black hole gravitational potential, or by polar outflow driven by radiation pressure? And is the velocity structure well ordered or randomised?

By modelling the line profile and differential phase data, we will measure the emission region size and construct a new radius-luminosity relationship. Our results can be compared with those obtained independently from reverberation techniques and used to constrain the physical origin of the atomic gas. We will also study the connection of the atomic gas to that of the hot dust continuum which we obtain using the same data (for example, GRAVITY Collaboration, 2019a & b). The angular size of both the hot dust and the atomic gas scales with optical flux, which makes interferometry well suited for studying luminous quasars like 3C 273 as well as nearby Seyfert galaxies. A future upgrade to the sensitivity of GRAVITY could further obtain kinematics, broad emission line region size, and black hole mass estimates for large samples out to a redshift $z \sim 2$.

Acknowledgements

This research was supported by Paris Observatory, Grenoble Observatory, by CNRS/INSU, by the *Programme National Cosmologie et Galaxies* (PNCG) of CNRS/INSU with INP and IN2P3, co-funded by CEA and CNES, by the *Programme National GRAM of CNRS/INSU* with INP and IN2P3, co-funded by CNES, by the *Programme National Hautes Energies* (PNHE) of CNRS/INSU with INP and IN2P3, co-funded by CEA and CNES, and by the *Programme National de Physique Stellaire* (PNPS) of CNRS/INSU, co-funded by CEA and CNES. It has also received funding from the following programmes: European Union's Horizon 2020 research and innovation programme (OPTICON Grant Agreement 730890), from the European Research Council (ERC) under the

European Union's Horizon 2020 research and innovation programme (Grant Agreement No. 743029), from the Irish Research Council (IRC Grant: GOIPG/2016/769) and SFI Grant 13/ERC/12907, from the Humboldt Foundation Fellowship and the ESO Fellowship programmes, from the European Research Council under the European Union's Horizon 2020 research and innovation programme (Grant Agreement Nos. 2016-ADG-74302 [EASY], 2015-StG-677117 [SFH], 694513, and 742095 [SPIDI]), and was supported in part by the German Federal Ministry of Education and Research (BMBF) under the grants *Verbundforschung* #05A08PK1, #05A11PK2, #05A14PKA and #05A17PKA, by *Fundação para a Ciência e a Tecnologia*, Portugal (Grants UID/

FIS/00099/2013, SFRH/BSAB/142940/2018 [P. G.] and PD/BD/113481/2015; M. F. in the framework of the Doctoral Programme IDPASC Portugal), by NSF grant AST 1909711, by the Heising-Simons Foundation 51 Pegasi b postdoctoral fellowship, from the *Direction Scientifique Générale of Onera* and by a Grant from Science Foundation Ireland under Grant number 18/SIRG/5597.

References

Peterson, B. M. et al. 2004, ApJ, 613, 682
Kaspi, S. et al. 2000, ApJ, 533, 631
Rakshit, S. et al. 2015, MNRAS, 447, 2420

GRAVITY Collaboration 2018, Nature, 563, 657
GRAVITY Collaboration 2019a, submitted to A&A, arXiv:1910.00593
GRAVITY Collaboration 2019b, submitted to A&A
Bentz, M. C. et al. 2013, ApJ, 767, 149
Du, P. et al. 2018, ApJ, 856, 6
Grier, C. J. et al. 2017, ApJ, 851, 21
Pancoast, A. et al. 2008, MNRAS, 445, 3073
Kishimoto, M. et al. 2011, A&A, 527, 121
Weigelt, G. et al. 2012, A&A Letters, 451, 9
Zhang, Z.-X. et al. 2019, ApJ, 876, 49

DOI: 10.18727/0722-6691/5167

An Image of the Dust Sublimation Region in the Nucleus of NGC 1068

GRAVITY Collaboration (see page 20)

The superb resolution of the Very Large Telescope Interferometer (VLTI) and the unrivalled sensitivity of GRAVITY have allowed us to reconstruct the first detailed image of the dust sublimation region in an active galaxy. In the nearby archetypal Seyfert 2 galaxy NGC 1068, the 2 μm continuum emission traces a highly inclined thin ring-like structure with a radius of 0.24 pc. The observed morphology challenges the picture of a geometrically and optically thick torus.

Introduction

NGC 1068 is one of the best studied nearby active galactic nuclei (AGN), in which accretion onto a central super-massive black hole contributes a significant fraction of the galaxy's total luminosity. The observation of broad polarised emission lines by Antonucci & Miller (1985) in the nucleus of this Seyfert galaxy was central to the development of the unified model that explains the differences between Seyfert 1 and Seyfert 2 objects as being due to the presence of a nuclear equatorial structure that both obscures and scatters the central emission depending on the line of sight.

Since the first seminal paper addressing its physical properties (Krolik & Begelman, 1988), and following numerous observations at many different wavelengths, the “torus” concept has evolved and been modified considerably. At the same time, increases in computational power have facilitated detailed modelling of clumpy torus structures. Such models are consistent with the near- to mid-infrared spectral energy distribution as well as dust reverberation measurements. Observations of almost two dozen galaxies using the MID-infrared Interferometric instrument (MIDI) on the VLTI have resolved the 1–3 pc scales where warm dust is responsible for the mid-infrared continuum (Burtscher et al., 2013 and references therein). However, measuring the size of the small (< 1 pc) region containing hot dust that emits at near-infrared wavelengths has been possible in very few galaxies. Also, until GRAVITY observed NGC 1068, there were no data showing spatial structure in this dust sublimation region.

Observations and Image Reconstruction

Data on NGC 1068 were obtained in November and December 2018 using GRAVITY and the four 8-metre UTs.

Under superb conditions, with seeing ~ 0.5 arcseconds and a coherence time of up to 13 ms, it was possible to fringe-track on the nucleus of NGC 1068 despite its large size and moderate brightness. The data obtained were of excellent quality, with typically < 1% visibility and closure-phase accuracy. The wealth of information provided by the six VLTI baselines has enabled us to reconstruct a *K*-band image based on the obtained closure phases and visibilities with 3-milliarcsecond (mas) resolution.

We used the publicly available Multi-aperture image Reconstruction Algorithm (MiRA; Thiébaud, 2008) to generate the image shown in Figure 1, which contains a total flux of 155 mJy. The structures present are robust, having been reproduced consistently over a wide variety of parameter settings, and with a signal level much higher than that expected for spurious sources. Full details are in GRAVITY Collaboration (2019).

A new view of NGC 1068

The image in Figure 1 is dominated by knots of continuum arranged in a ring around a central hole, with the south-western side about a factor of two brighter than the north-eastern side. Fitting an